BBAA VI International Colloquium on:
Bluff Bodies Aerodynamics & Applications
Milano, Italy, July, 20-24 2008

MEASUREMENTS ON THE SURFACE WIND PRESSURE CHARACTERISTICS OF TWO SQUARE BUILDINGS UNDER DIFFERENT WIND ATTACK ANGLES AND BUILDING GAPS

Bao-Shi Shiau [*,†], Ho-Chieh Chang [†]

[*]Institute of Physics
Academia Sinica, Taipei, 115, Taiwan
e-mail: bsshiau@gate.sinica.edu.tw

[†] Department of Harbor and River Engineering
National Taiwan Ocean University, Keelung, 202, Taiwan
e-mails: b0085@mail.ntou.edu.tw

Keywords: surface wind pressure, pressure spectrum, probability density function.

Abstract. *Measurements of the surface wind pressure statistical characteristics and pressure spectrum of two square buildings in side by side arrangement with various gaps and under different wind attack angles are performed in wind tunnel. Effects of the building gap and wind attack angle on the characteristics of wind pressure for the inner face and front face of two buildings are reported in the study. Results are: (1) For the inner faces of buildings at height Z/H=0.888, and wind attack angle 0^o, the mean wind pressure coefficients are all negative value. And the mean wind pressure coefficient decreases as increasing the downstream distance X/W, in general. When the building gap decreases, the absolute value of mean wind pressure coefficient becomes larger. (2) For the inner faces and front faces of buildings at height Z/H=0.888, and building gap D/W=0.5, the mean surface wind pressure increases as the wind attack angle increases. The root mean square of pressure fluctuation becomes smaller at a longer downstream distance. At the nearer downstream distance, the root mean square of pressure fluctuation becomes larger, especially for the wind attack angles within 15^o and 30^o. The variation of root mean square of pressure fluctuation exhibits the trend of decrease when the wind attack angle is increasing. (3)The power spectra of surface wind pressure fluctuation for various building gaps at z/H=0.888, y/W=0.38 of building I and wind attack angle 0^o are shown to have the slope of -5/3 at the inertia subrange of the spectra distribution. It is similar to the Kolomogrov turbulent velocity spectrum law. Also the peak value of the power density of fluctuating pressure is reduced as the wind attack angle increases. And the decay slope of power spectra curve at the inertia subrange becomes slowly as the wind attack angle change from 0^o to 30^o. (4) The peak values of the probability density functions of the surface wind pressure fluctuation for different heights in front face of buildings are all close to 0.4. At the lowest height location, the skewness coefficient of the probability density function for pressure fluctuation becomes the largest.*

1 INTRODUCTION

It has been frequently suffered typhoon's serious attacks during summer and autumn seasons in Taiwan. Strong winds caused severe damage on high-rise building cladding. Also, surface wind pressure distributions affect the building natural ventilation. For this purpose, it is necessary to study the building surface wind pressure characteristics which can provide more accurate and detail information for the building wall curtain cladding and natural ventilation designs.

Previous studies, like [1, 2, 3] only studied on one building. In urban city, two buildings of side by side arrangement are commonly encountered [4]. The wind attack angle on the buildings also often changed in time. Therefore the objective of present study is to measure in wind tunnel the surface wind pressure characteristics and pressure spectrum of two square buildings in side by side arrangement with various gaps and under different wind attack angles.

2 EXPERIMENTAL SET-UP

The experiments were conducted in the Environmental Wind Tunnel of National Taiwan Ocean University. The test section of the wind tunnel had a cross section of 2 m by 1.4 m with 12.5 m long. The wind tunnel was an open suction type and it contracted to the test section with an area ratio of 4: 1. The turbulence intensity of the empty wind tunnel is less than 05 % at the free stream velocity of 5 m/s.

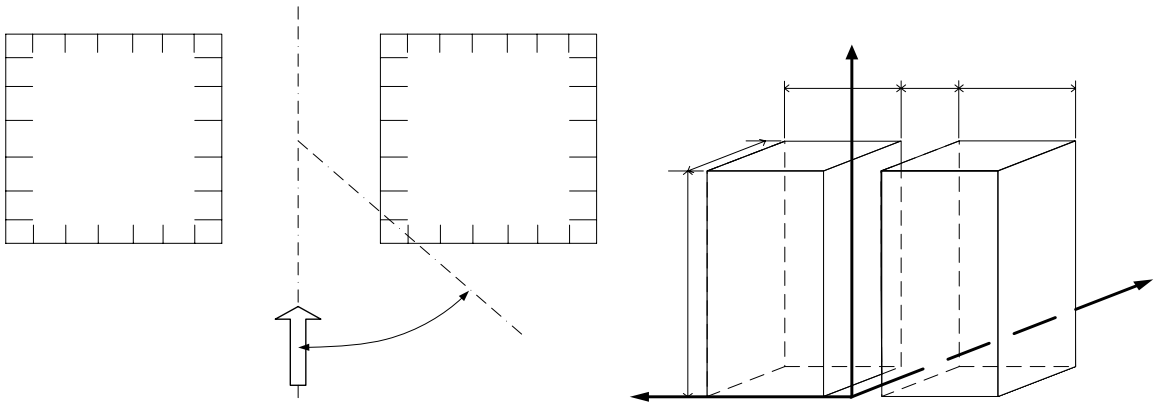

Figure 1 Schematic diagram of two building models arrangement

Four spires and roughness elements are arranged on the entrance of test section to simulate a neutral atmospheric boundary layer flow in urban region. Two square models are arranged in side by side with different gaps (see Fig.1). Each square model is 10 cm by 10 cm, and 25 cm high. The model is at a scale of 1 to 500. Fig 1 shows the arrangement of two buildings models in the wind tunnel. And labels of pressure taps on two building models are shown in the Fig.1

The X-type hot-wire incorporating with the TSI IFA-300 constant temperature anemometer was used to measure the turbulent flow signals. Output of the analog signals for turbulent flow was digitized at a rate of 4 K Hz each channel through the 12 bit Analog-to–Digital converter. Since none of the analog signals containing significant energy or noise above 1 K Hz, with the Nyquist criteria, a digitizing rate of 2 K Hz was sufficient. The low pass frequency for the analog signals is set as 1 K Hz in all runs of the experiments.

The surface wind pressure was measured by using the HyScan-2000 scanning system of the Scanivalve corporation. The system includes a pressure calibration module SPC-3000, and

a control pressure module CPM-3000. Pressure was measured by using the ZOC-23B pressure transducer that has 32 channels. The CSM-2000 unit receives many address information from the IFM2000 module and distributes it to the cable-serviced ZOC-23B modules, then routes the addressed analog signals back to the IFM2000 module. The IFM2000 module is the interface unit for ZOC-23B. The DAQ2000 is the self-contained high speed data acquisition and processing system. The HyScan-2000 system incorporating with the DAQ2000 can sample 16~32 channels of the pressure transducer analog data. In the present study, we sampled 24 channels almost simultaneously at the sampling rate of 2000 Hz and took the sampling time 32.468 seconds for each run.

3 APPROACHING FLOW

3.1 Mean velocity profile

The urban terrain type of neutral turbulent boundary layer was generated as the approaching flow. Mean velocity profile of the simulated turbulent boundary layer flow is approximated by the power law.

$$\frac{U(Z)}{U_{ref}} = (\frac{Z}{Z_{ref}})^n \tag{1}$$

where *U(Z)* is the mean velocity at height of Z , U_{ref} is the free stream velocity, and Z_{ref} is the boundary layer thickness.

In the present study, an urban terrain type of neutral atmospheric boundary layer was simulated with a model scale of 1/500. The free stream velocity is 12 m/s; and the boundary layer thickness, Z_{ref} is about 100 cm. The measured mean velocity profile is shown in Fig.2. Results of simulation indicate that the power exponent *n* is 0.279. This value lies in the range of 0.23 to 0.40 as proposed by Counihan [5] for the urban terrain type of neural atmospheric boundary layer flow.

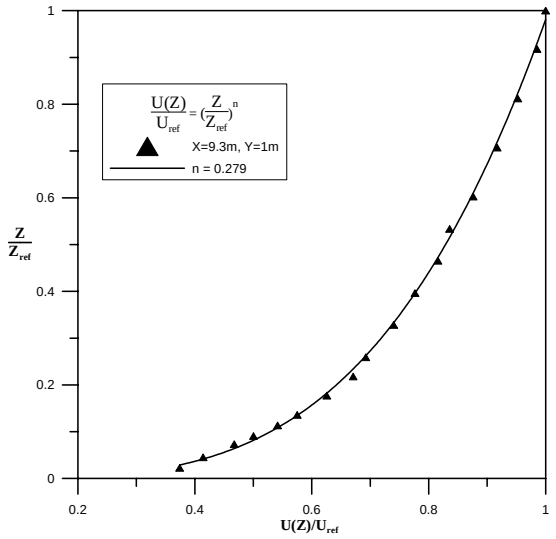

Figure2 Mean velocity profile of approaching flow

3.2 Turbulence intensity profile

The simulated turbulence intensity profile is shown in Fig.3. It is seen that the simulated longitudinal turbulence intensity close to the wall is about 21%. Counihan [5] had found that

the longitudinal turbulence intensity close to the ground in the urban terrain areas fell in the range of 20% to 35 %.

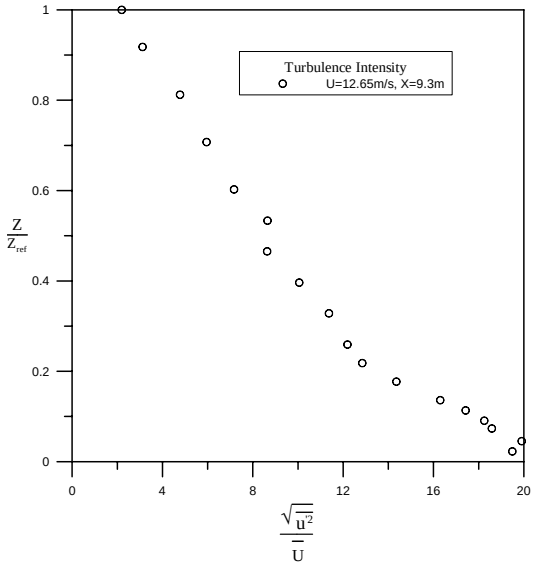

Figure 3 Turbulence intensity profile of approaching flow

4 MEASUREMENT RESULTS OF SURFACE WIND PRESSURE

Measurement data were analyzed to obtain the mean surface wind pressure coefficient, $\overline{C_p}$, and root mean square of pressure fluctuation coefficient, C_{prms}. The analysis for power spectrum and probability density function of wind pressure fluctuation were also reported.

4.1 Effect of building gap on the wind pressure of inner faces of two buildings

It is interesting to investigate the building gap affecting the surface wind pressures of the two inner faces of buildings. Measurement results of Shiau and Lai [4] revealed that the maximum negative wind pressure occurred about at the height of Z/H=0.888 for the inner faces of two buildings. So we chose this location for analysis.

Fig.4 shows the variations of the mean wind pressure on inner faces of two buildings at height Z/H=0.888 for different building gaps, D/W, with wind attack angle 0^o. Results indicate that the mean wind pressure coefficients are all negative. The mean wind pressure coefficient decreases as increasing the downstream distance X/W, in general. When the building gap decreases, the absolute value of mean wind pressure coefficient becomes larger. The variations of the root mean square of wind pressure fluctuation on inner faces of two buildings at height Z/H=0.888 for different building gaps, D/W, with wind attack angle 0^o are shown in Fig.5. Roughly speaking, for 0< X/W< 0.45, the C_{prms} value is larger for the case of gap D/W=05 than that of D/W=1.0 and 3.0. But for 0.45< X/W< 1.0, C_{prms} value is smaller for the case of gap D/W=0.5 than that of D/W=1.0 and 3.0.

4.2 Effect of wind attack angle on the wind pressure of inner and outer faces of two buildings

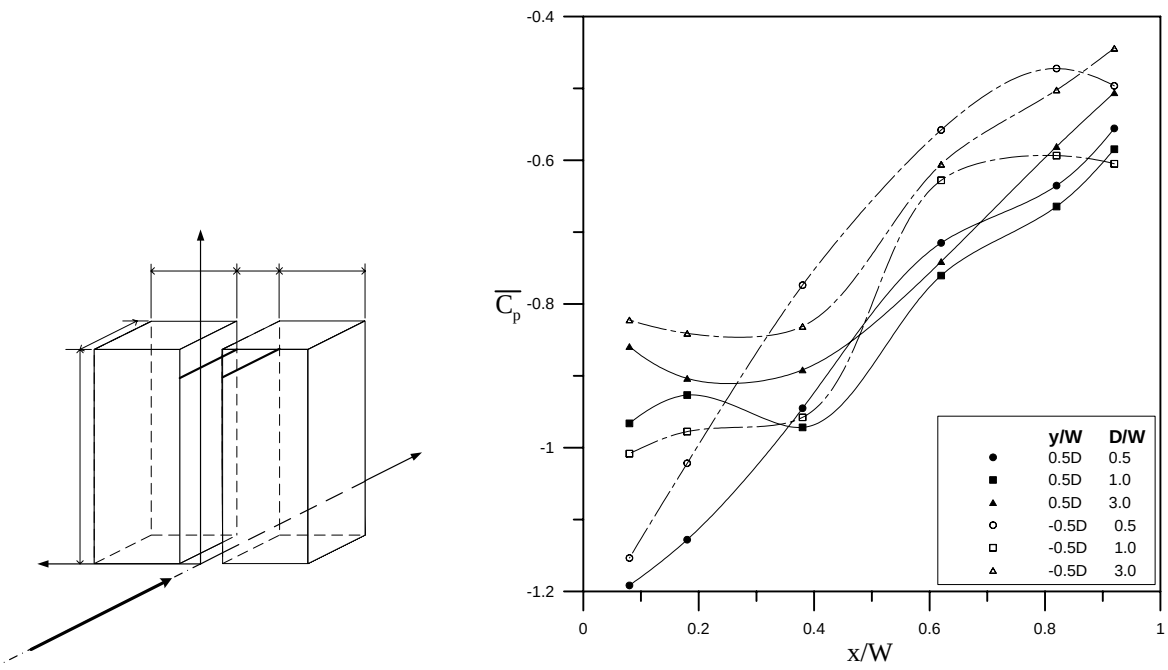

Figure 4 Variation of the mean wind pressure on inner faces of two buildings at height Z/H=0.888 for different building gaps, D/W, with wind attack angle 0^o

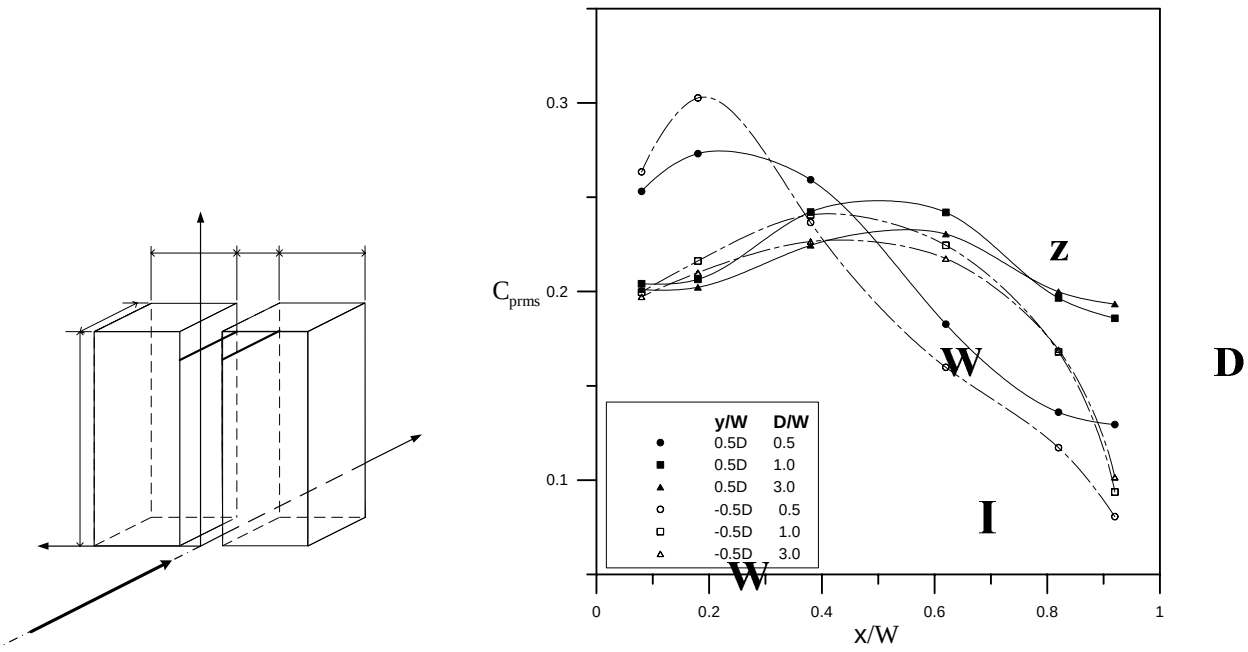

Figure 5 Variation of root mean square of wind pressure fluctuation on inner faces of two buildings at height Z/H=0.888 for different building gaps, D/W, with wind attack angle 0^o

For the inner faces of buildings at height Z/H=0.888, and building gap D/W=0.5, the mean and root mean square of surface wind pressure variations for different wind attack angles are shown in Fig. 6 and Fig.7. Results reveal that the mean surface wind pressure increases as the wind attack angle increases. The root mean square of pressure fluctuation becomes smaller at a longer downstream distance. At the nearer downstream distance, the root mean square of

pressure fluctuation becomes larger, especially for the wind attack angles within 15^o and 30^o. The variation of root mean square of pressure fluctuation exhibits the trend of decrease when the wind attack angle is increasing.

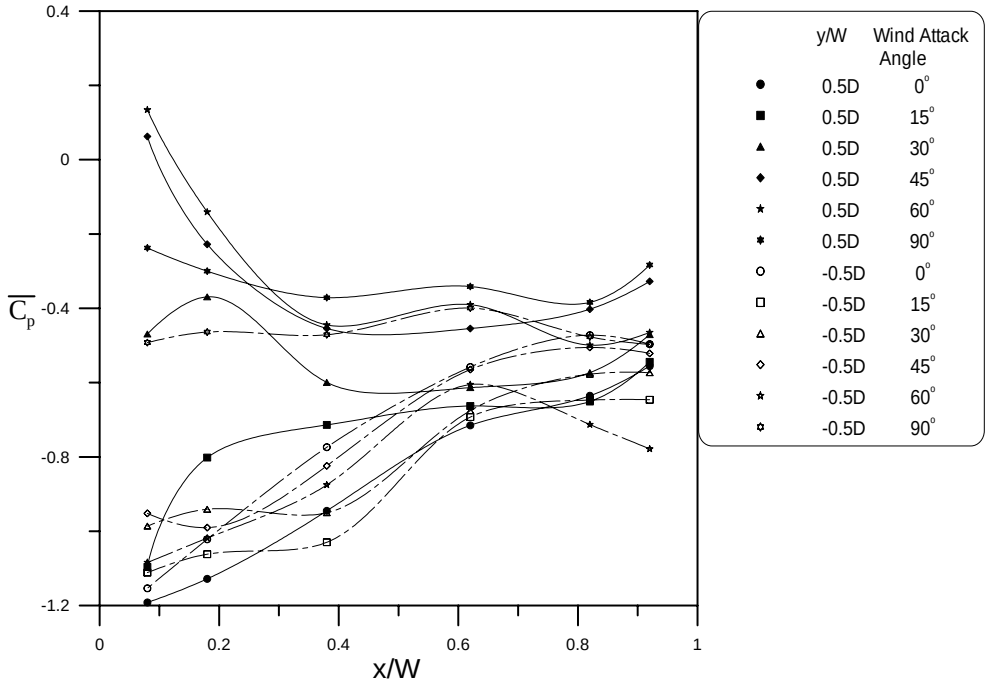

Figure 6 Mean wind pressure variations for different wind attack angles at inner face of building height of Z/H=0.888, and building gap D/W=0.5

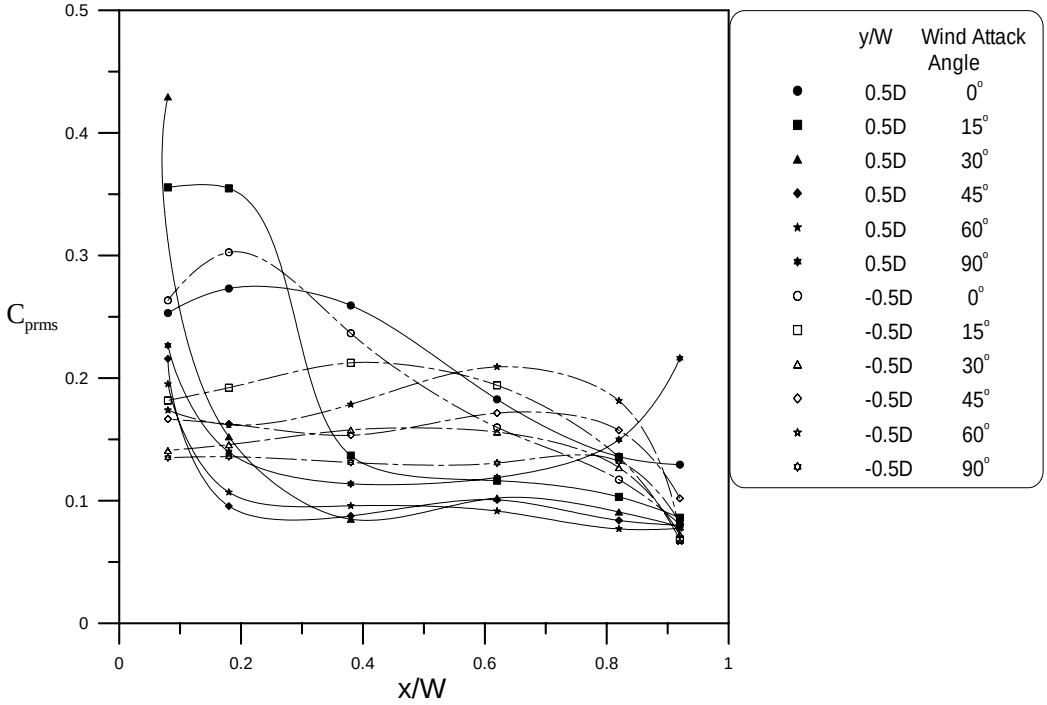

Figure 7 Root mean square of wind pressure variations for different wind attack angles at inner face of building height of Z/H=0.888, and building gap D/W=0.5

For front faces of buildings at height Z/H=0.888, and building gap D/W=0.5, the mean and root mean square of surface wind pressure variations for different wind attack angles are shown in Fig. 8 and Fig.9. Results reveal that the mean surface wind pressure increases as the wind attack angle increases. The root mean square of pressure fluctuation becomes smaller at a longer downstream distance. At the nearer downstream distance, the root mean square of pressure fluctuation becomes larger, especially for the wind attack angles within 15^o and 30^o. The variation of root mean square of pressure fluctuation exhibits the trend of decrease when the wind attack angle is increasing.

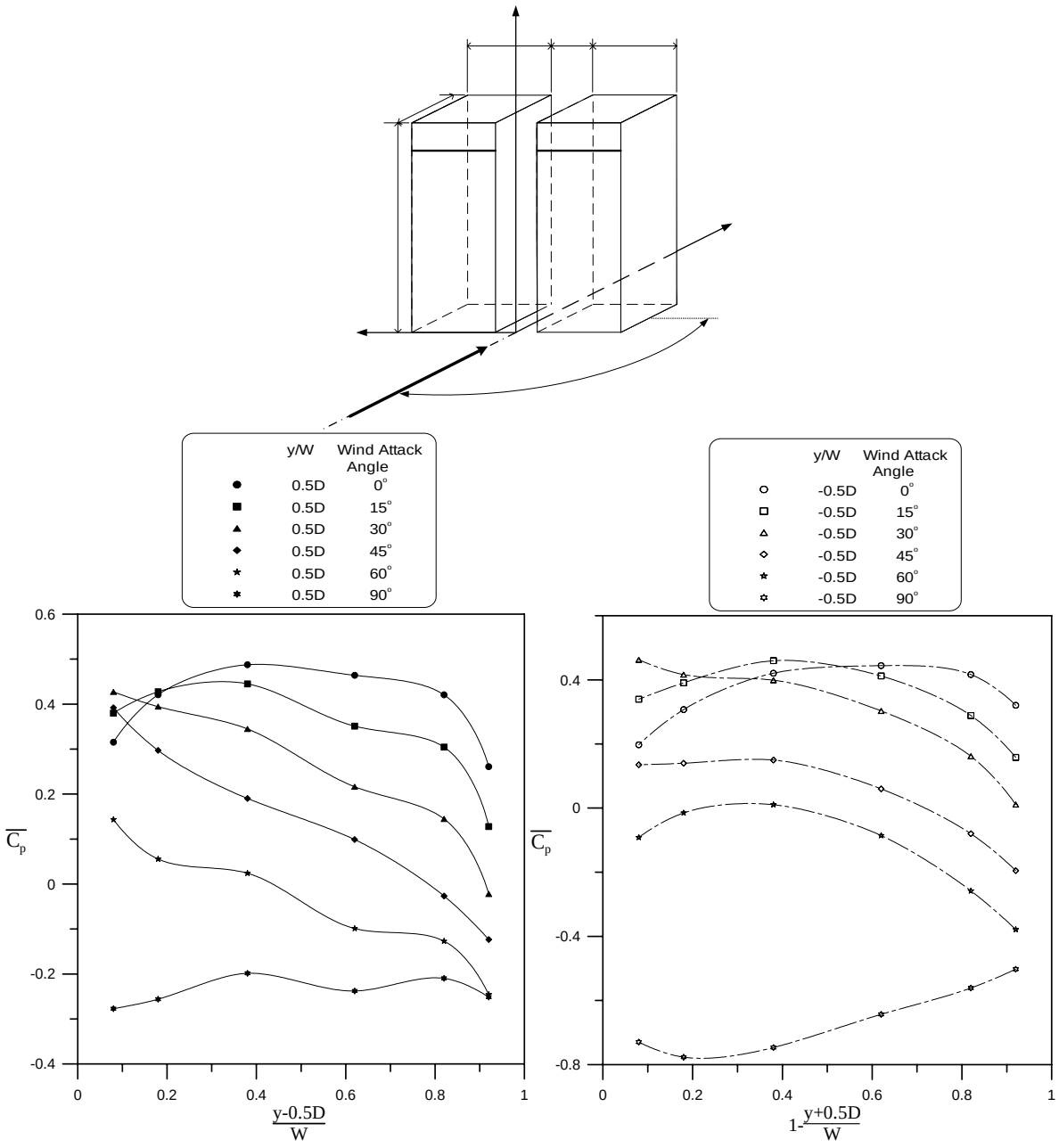

Figure 8 Mean wind pressure variations for different wind attack angles at front face of building height of Z/H=0.888, and building gap D/W=0.5

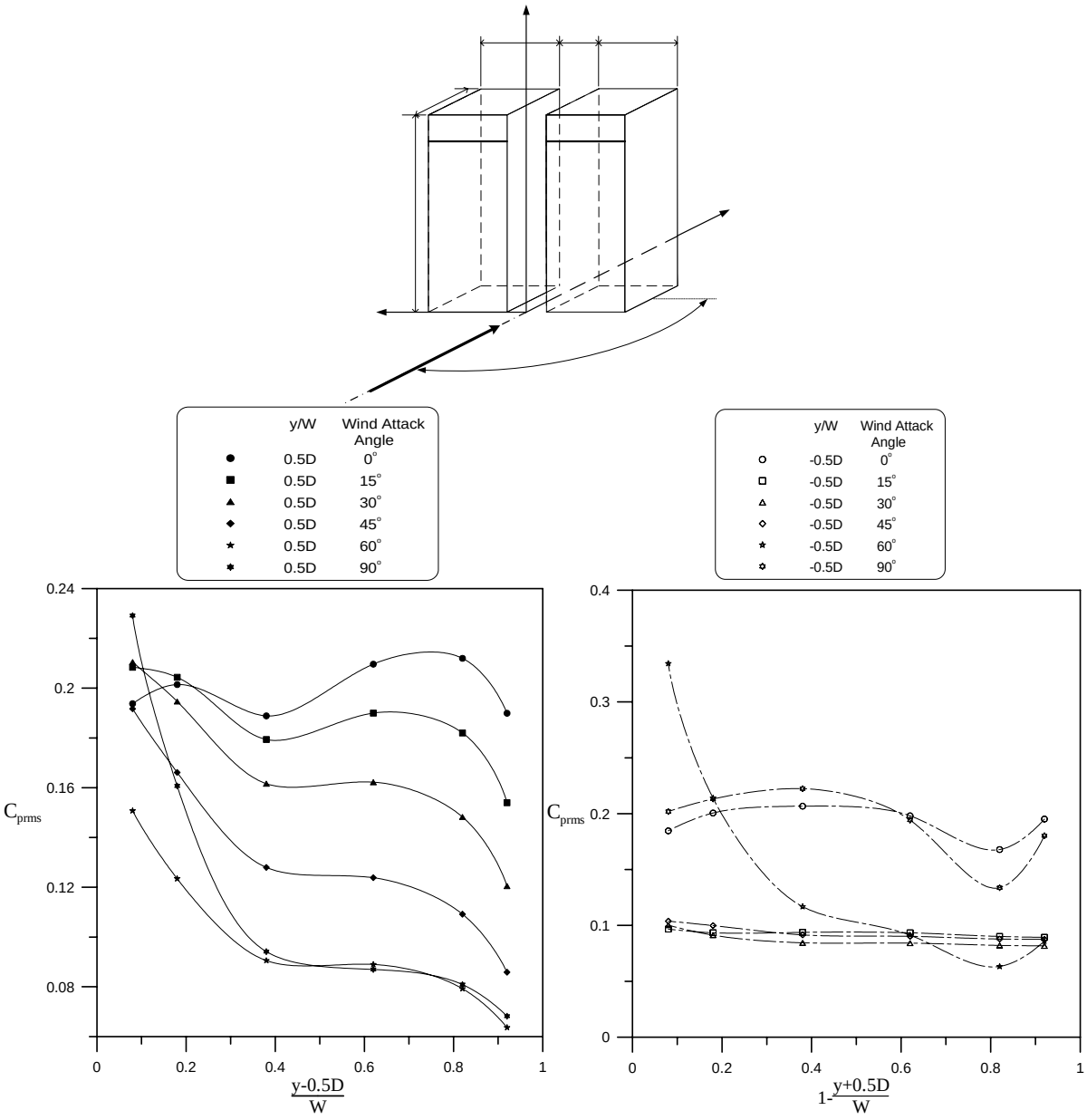

Figure 9 Root mean square of wind pressure variations for different wind attack angles at front face of building height of Z/H=0.888, and building gap D/W=0.5

4.3 Power spectrum of the wind pressure fluctuation

The power spectrum of wind pressure fluctuation for various building gaps at z/H=0.888, y/W=0.38 of Building I and wind attack angle 0^o shown in Fig.10. The spectra distributions all exhibit with the curve slope of -5/3 at the inertia subrange, which is similar to the Kolo-mogrov turbulent velocity spectrum law [6]. Kumar and Stathopoulos [7] investigated the power spectra of wind pressure on low building roofs. They obtained a similar result of decay law of power spectra.

As wind attack angle increases to 30^o, the power spectrum of wind pressure fluctuation for various building gaps at z/H=0.888, y/W=0.38 of Building I are presented on Fig.11. When we compare Fig.10 and Fig.11, The peak value of the power density of fluctuating pressure is

reduced as the wind attack angle increases. And the decay slope of power spectra curve at the inertia subrange becomes slowly as the wind attack angle change from 0^o to 30^o.

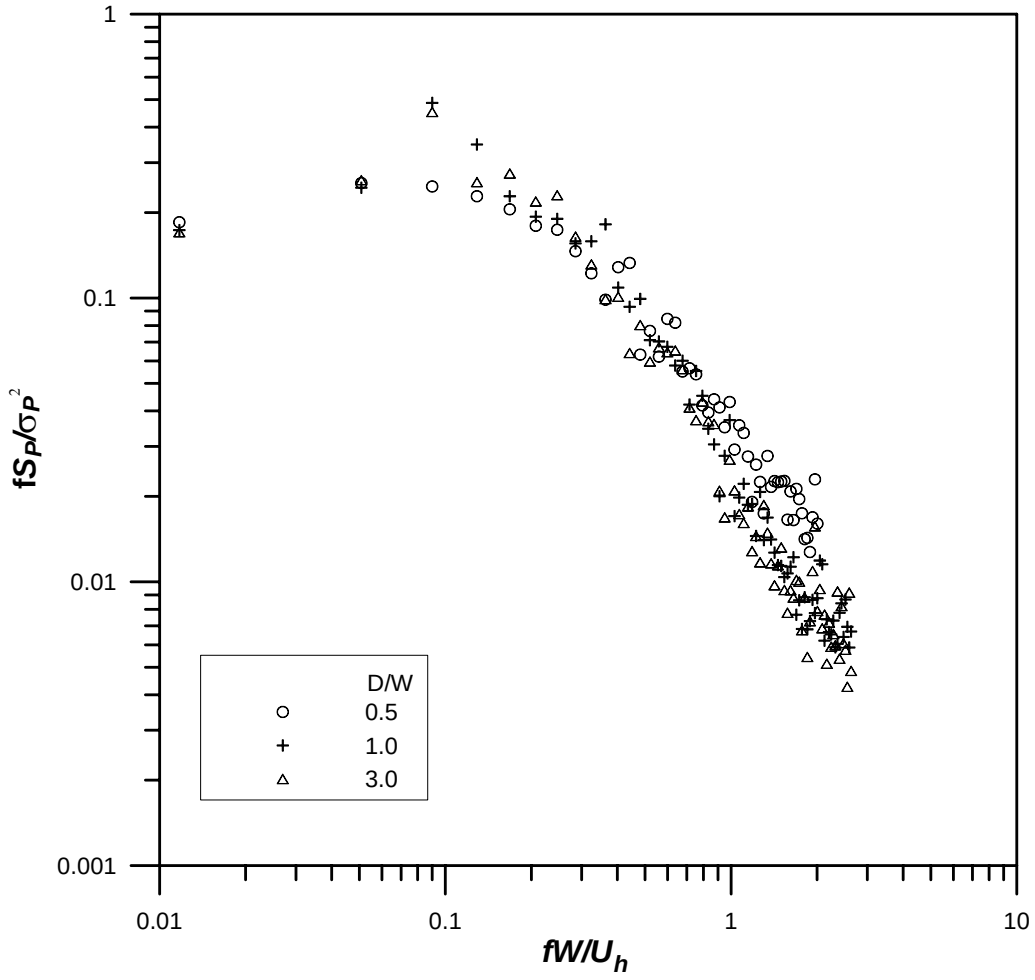

Figure 10 Power spectrum of wind pressure fluctuation for various building gaps at z/H=0.888, y/W=0.38 of Building I and wind attack angle 0^o

4.4 Probability density function of fluctuating wind pressure

For assessing the design of cladding and glass panels of buildings and structures, it is required to have full knowledge of the probability distribution of fluctuating pressure. The nature of fluctuating wind pressure is revealed by its probability density function (PDF). And the PDF is characterized by parameters, such as reduced parameter g , skewness coefficient, S_k and kurtosis coefficient, K_u , which are defined, respectively, as:

$$g = (p_i - \overline{p}) \big/ \sigma_p \tag{2}$$

$$S_u = [\sum_1^n (p_i - \overline{p})^3 / n] / \sigma_p^3 \tag{3}$$

$$K_u = [\sum_1^n (p_i - \overline{p})^4 / n] / \sigma_p^4 \tag{4}$$

where p_i is the instantaneous wind pressure, $\overline{p}$ is the mean wind pressure, n is the data numuber, and σ_p is the standard deviation of wind pressure distribution.

$$\sigma_p = [\sum_{1}^{n} (p_i - \overline{p})^2 / n]^{1/2} \tag{5}$$

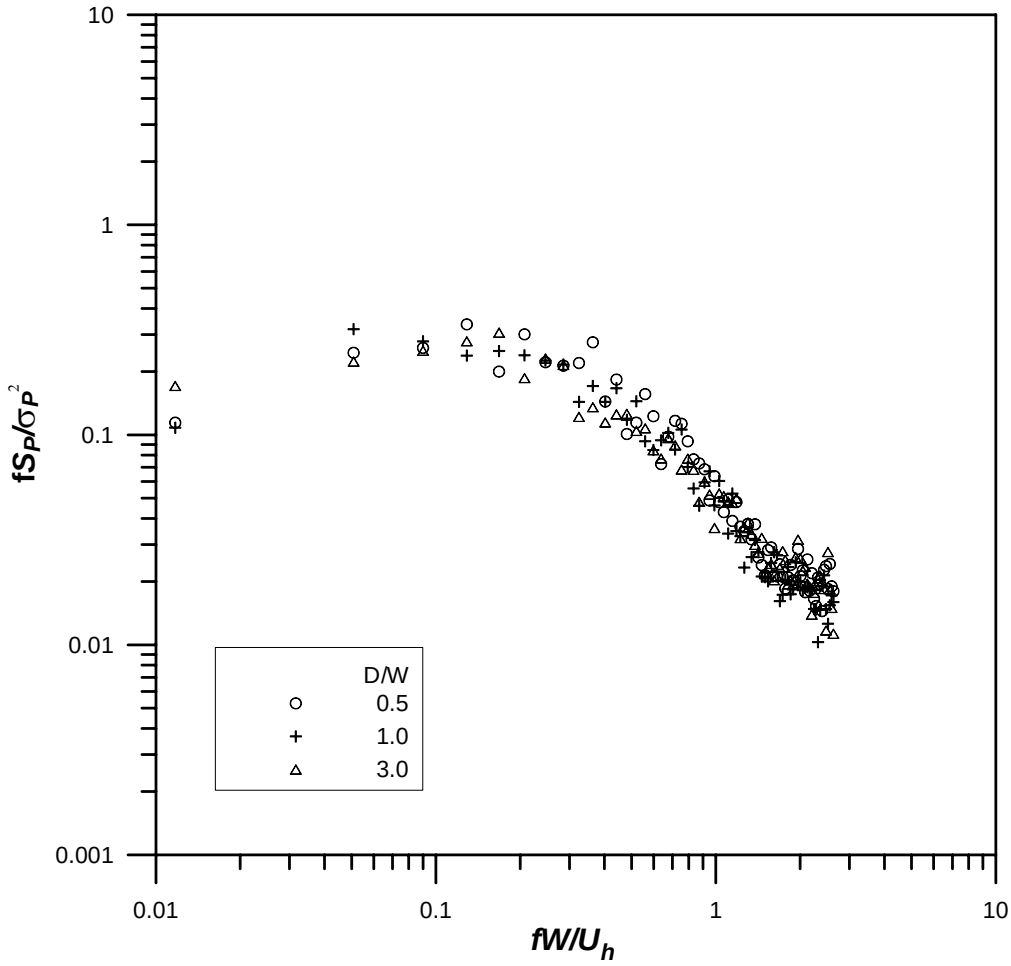

Figure 11 Power spectrum of wind pressure fluctuation for various building gaps at z/H=0.888, y/W=0.38 of Building I and wind attack angle 30°

Figure 12 is the probability density functions of fluctuating pressure variations for different heights of Building I, at y/W=0.35, with wind attack angles 0°, and building gap D/W=3.0. Results show that the peak values of the probability density functions of the surface wind pressure fluctuation for different heights in front face of buildings are all close to 0.4. At the lowest height location, the skewness coefficient, S_k of the probability density function for pressure fluctuation becomes the largest. The value of S_k in all heights are positive. They correspond to skewness to the right.

Figure 13 shows the probability density function of fluctuating pressure variations along downwind direction for inner face of buildings at height of Z/H=0.888, wind attack angles 0°, and building gap D/W=0.5. The shapes of measured PDF curves shown in Fig.13 all exhibit skew. The peak value of the PDF for Gaussian distribution is 0.4. And the skewness coefficient and kurtosis coefficient for Gaussian distribution are equal to 0 and 3, respectively. All the skewness coefficients shown in the Fig.13 are all not equal 0 and with $S_k < 0$. They corre-

spond to the PDF is skew to the left. As increasing building gap to D/W=3.0, PDF for inner face of buildings at height of Z/H=0.888, wind attack angles 0^o, is shown in Fig.14. The skewness coefficients for the PDF shown in figure are also all negative values. Li et al. [8] measured PDF in the separated and reattaching flow of building also obtained similar results.

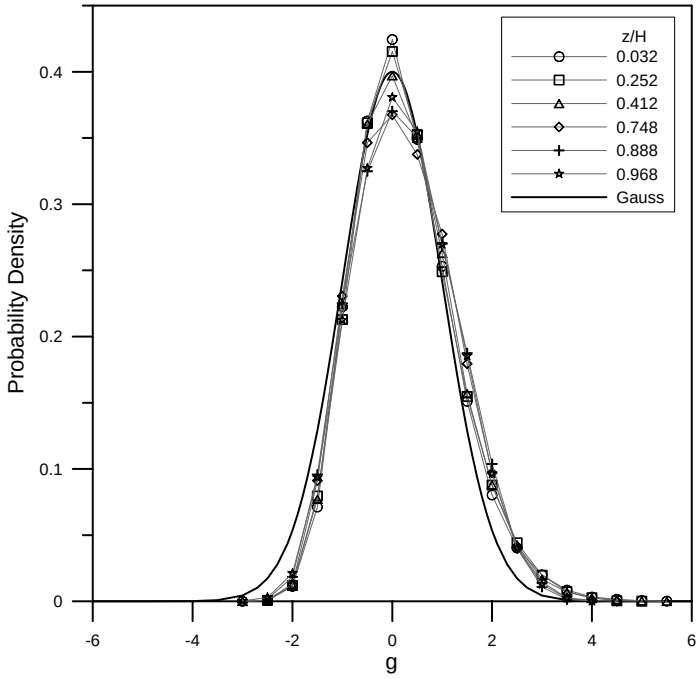

Figure 12 Probability density function of fluctuating pressure variations for different heights of Building I, at y/W=0.35, with wind attack angles 0^o, and building gap D/W=3.0.

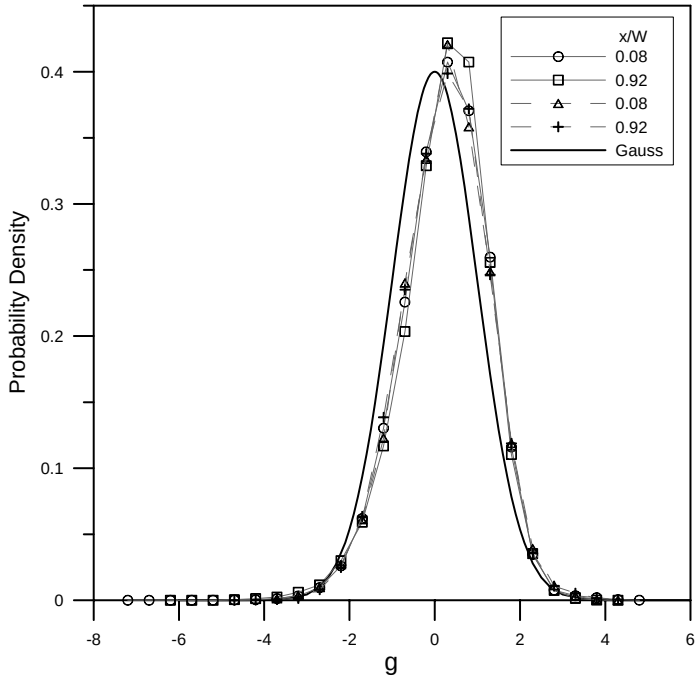

Figure 13 Probability density function of fluctuating pressure variations along downwind direction for inner face of buildings at height of Z/H=0.888, wind attack angles 0^o, and building gap D/W=0.5. (○,□:Building I; △, +:Building II)

The probability density functions for different wind attack angles with Building II of outer face at the height Z/H=0.888, X/W=0.92, and D/W=3.0 are shown in Fig.15. As the wind attack angle changes to 90^o, the outer face of Building II becomes front face. So the shape of PDF of fluctuating pressure close to Gaussian distribution, accordingly.

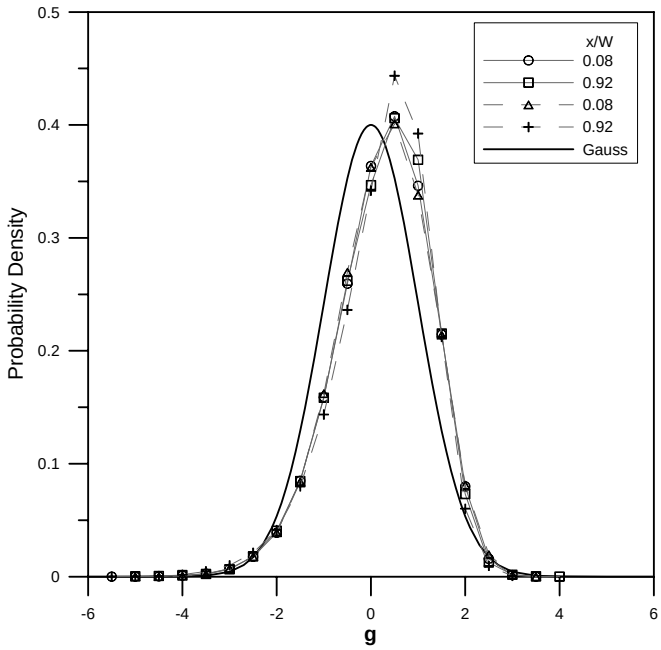

Figure 14 Probability density function of fluctuating pressure variations along downwind direction for inner face of buildings at height of Z/H=0.888, wind attack angles 0^o, and building gap D/W=3.0. (○,□:Building I; △, +:Building II)

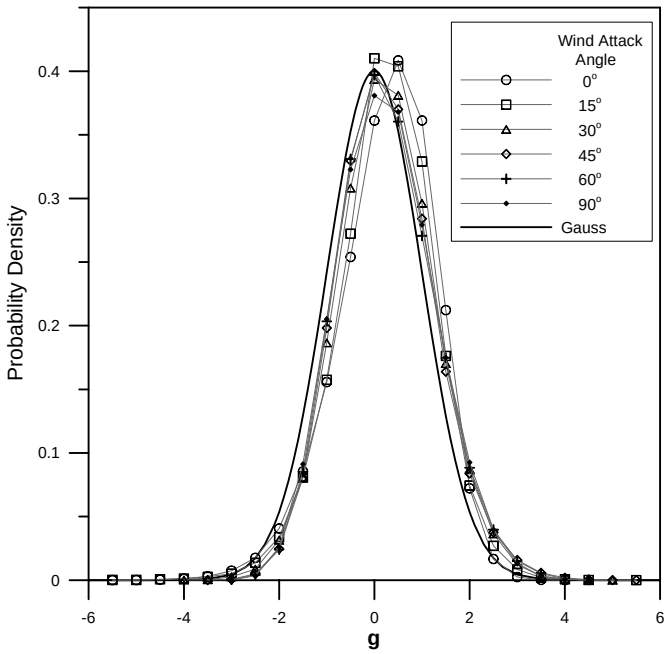

Figure 15 The probability density functions for different wind attack angles with Building II of outer face at the height Z/H=0.888, X/W=0.92, and D/W=3.0

5 CONCLUSIONS

Measurements of the surface wind pressure characteristics and pressure spectrum of two square buildings in side by side arrangement with various gaps and under different wind attack angles are performed in wind tunnel. Results of the analysis of the measurement data are summarized as follows:

- For the inner faces of buildings at height Z/H=0.888, and wind attack angle 0^o, the mean wind pressure coefficients are all negative value. And the mean wind pressure coefficient decreases as increasing the downstream distance X/W, in general. When the building gap decreases, the absolute value of mean wind pressure coefficient becomes larger.
- For the inner faces and front faces of buildings at height Z/H=0.888, and building gap D/W=0.5, the mean surface wind pressure increases as the wind attack angle increases. The root mean square of pressure fluctuation becomes smaller at a longer downstream distance. At the nearer downstream distance, the root mean square of pressure fluctuation becomes larger, especially for the wind attack angles within 15^o and 30^o. The variation of root mean square of pressure fluctuation exhibits the trend of decrease when the wind attack angle is increasing.
- The power spectra of surface wind pressure fluctuation for various building gaps at z/H=0.888, y/W=0.38 of building I and wind attack angle 0^o are shown to have the slope of -5/3 at the inertia subrange of the spectra distribution. It is similar to the Kolomogrov turbulent velocity spectrum law. Also the peak value of the power density of fluctuating pressure is reduced as the wind attack angle increases. And the decay slope of power spectra curve at the inertia subrange becomes slowly as the wind attack angle change from 0^o to 30^o.
- The peak values of the probability density functions of the surface wind pressure fluctuation for different heights in front face of buildings are all close to 0.4. At the lowest height location, the skewness coefficient of the probability density function for pressure fluctuation becomes the largest.

REFERENCES

[1] J.P. Huot, C. Rey, and H. Arbey, Experimental Analysis of the Pressure Field Induced on Square Cylinder by a Turbulent Flow, Journal of Fluid Mechanics, **162**, 283-298, 1986.

[2] J. Wacker, Local Wind Pressure for Rectangular Buildings in Turbulent Boundary Layers, Wind Climate in Cities, 185-207, 1995.

[3] Y. Uematsu, and N. Isyumov, Wind Pressures Acting on Low-Rise Buildings, Journal of Wind Engineering & Industrial Aerodynamics, Vol.**82**, 1-25, 1999.

[4] B. S Shiau, and J. H Lai, Experimental Study on the Surface Wind Pressure and Spectrum for Two Prismatic Buildings of Side by Side Arrangement in a Turbulent Boundary Layer Flow, Proceedings of the 6^{th} Asia-Pacific Conference on Wind Engineering, 303-317, Seoul, Korea, 2005

[5] J. Counihan, Adiabatic Atmospheric Boundary Layers: A Review and Analysis of Data from the Period 1880-1972, Atmospheric Environment, Vol.9, pp. 871-905, 1975

[6] Cesar Farell and Arun K.S. Iyengar ,Experiments on the Wind Tunnel Simulation of Atmospheric Boundary Layers, Journal of Wind Engineering & Industrial Aerodynamics, Vol.**79**, 11-35, 1999.

[7] K. Suresh Kumar, and T. Stathopoulos, Power Spectra of Wind Pressures on Low Building Roofs, Journal of Wind Engineering and Industrial Aerodynamics, Vol.74-76, pp.665-674, 1998

[8] Q.S. Li, I. Calderone, and W.H. Melbourne, Probabilistic Characteristics of Pressure Fluctuations in Separated and Reattaching Flows for Various Free-Stream Turbulence, Journal of Wind Engineering and Industrial Aerodynamics, Vol.82, pp.125-145, 1999